

# Physics of Josephson Junctions Made of High- $T_c$ Superconductors

*M. Yu. Kupriyanov*

Department of Physics, Moscow State University, 119899 Moscow, Russia

**Abstract.** The main results achieved in the HTS Josephson junction technology are reviewed and the possible reasons leading to the reduction of their characteristic voltage are discussed. It is emphasized that the electron diffraction at the SN boundaries as well as at the inhomogeneities in CuO planes plays a decisive role in HTS weak links and grain boundary junctions.

## 1. Introduction

So far the possibility of making HTS Josephson junctions with the value of the characteristic voltage as high as  $V_c \simeq 20 - 30$  mV at  $T = 4.2$  K have been proven experimentally in the monocrystalline break junctions [1]. But till now all attempts to develop a way to fabricate reproducible HTS weak links [2-8] or single grain boundary junctions [9-12] with the same characteristics have never led to a noticeable success.

The goal of this work is to review possible mechanisms leading to the  $V_c$  suppression in HTS Josephson junctions and to discuss their relevance to the experimental data.

## 2. Josephson effect in HTS weak links

The calculations in the BCS based weak link models [13,14] show that their properties depend on two dimensionless parameters which in the "dirty" limit given by the equalities

$$\gamma = \rho_S \xi_S^* / \rho_N \xi_N^*, \quad \gamma_B = R_B / \rho_N \xi_N^* \quad (1)$$

where  $\rho_{N,S}$  and  $\xi_{N,S}^*$  are the normal-state resistivities of the junction materials, and their coherence lengths respectively, while  $R_B$  is the specific resistance of the SN boundary.

The characteristic voltage  $V_c$  of SNS sandwich-type junctions in the limits of small thickness of the junction  $L \ll \xi_N^*$  or large  $\gamma_B \gg \max\{(T_c/T)^{1/2}, \gamma(1 - T/T_c)^{-1/2}\}$  is given by equations (2) and (3) respectively:

$$\frac{eV_c}{2\pi T_c} = \frac{T}{T_c} \max_{\phi} \sum_{\omega > 0} \frac{\Delta^2 G_S \omega^{-1} \sin(\phi)}{\sqrt{\omega^2 (1 + \gamma_{BM} \omega G_S / 2\pi T_c)^2 + \Delta^2 \cos^2(\phi/2)}} \quad (2)$$

$$\frac{eV_c}{2\pi T_c} = \frac{2}{\gamma_B} \sum_{\omega > 0} \frac{\Delta^2}{\omega^2 + \Delta^2} \sqrt{\frac{\pi T^2}{\omega T_c}} \text{sh}^{-1} \left[ \frac{L}{\xi_N^*} \sqrt{\frac{\omega}{\pi T_c}} \right], \quad (3)$$

where  $\phi$  is the phase difference of the superconductor order parameters,  $\omega = \pi T(2n + 1)$  are the Matsubara frequencies,  $G_S = \omega \sqrt{\omega^2 + \Delta^2}$ ,  $\gamma_{BM} = \gamma L / \xi_N^*$ ,  $L$  is the thickness of the N-layer. The specific normal junction resistance is determined by the sum of the interface resistances:

$$R_N = 2\xi_N^* \rho_N \gamma_B. \quad (4)$$

In the SN-N-NS variable thickness bridges the SN interface resistances also make a noticeable contribution to the full junction resistance  $R_N$  :

$$R_N = 2\xi_N^* \rho_N \gamma_{BM}^{1/2}, \quad \gamma_{BM} = \gamma d_N / \xi_N^*, \quad (5)$$

where  $d_N$  is the thickness of the N-film. The temperature dependencies of the parameter  $V_c$  in the cases of large  $\gamma_{BM} \gg T_c/T$  or small bridge length  $L$

$$L \ll \max\{\xi_N^*, \xi_N^* \sqrt{\gamma_{BM}} \min\{1, \sqrt{T/(T_c(1 + \gamma_{BM}))}\}\}$$

are determined by equations (6) and (7) respectively:

$$\frac{eV_c}{2\pi T_c} = \frac{T}{T_c} \sum_{\omega > 0} \frac{\Delta^2}{\omega^2 + \Delta^2} \left( \frac{\pi T_c}{\omega \gamma_{BM}} \right)^{3/2} \exp\left( - \frac{L}{\xi_N^*} \sqrt{\frac{\omega}{\pi T_c}} \right), \quad (6)$$

$$\frac{eV_c}{2\pi T_c} = \frac{T}{T_c} \max_{\phi} \sum_{\omega > 0} \Delta^2 \sin(\phi) [2\Omega_c^2 \Omega (\Omega + \Omega_c^2)]^{-1/2} \quad (7)$$

where  $\Omega = \sqrt{\omega^2 + \Delta^2}$ ,  $\Omega_c = \omega \sqrt{(1 + \gamma_{BM} \Omega / \pi T_c)^2 + \Delta^2 \cos^2(\phi/2)}$ .

Expressions (2)-(7) are valid if the conditions of dirty limit are fulfilled for N- and S-metals as well as the suppression of the superconductivity in the S electrodes of the structures due to both the proximity effect and the supercurrent flow is negligible.

To use those results for HTS weak links one should also suppose that in HTS material the mean-field approximation holds and the weak coupling limit takes place. The first condition is probably satisfied in the HTS due to the smallness of the ratio  $T_c/E_f$  [15]. Since the experimentally obtained  $\Delta(T)$  dependence is similar to that predicted by the BCS theory the account of strong-coupling effects results only in a modification of the ratio  $\Delta(0)/T_c$  and can result in temperature independent corrections to  $V_c$  of the order of unity.

Rough estimations [14] of the suppression parameters for the atomically sharp and "clean" (without additional dielectric layers) HTS/N-interface give

$$\gamma_{\perp} \simeq 10^2, \gamma_{B\perp} \simeq 10^4, \quad (8)$$

if the C axis of HTS material is perpendicular to the SN boundaries of the junctions and

$$\gamma_{\parallel} \simeq 5, \gamma_{B\parallel} \simeq 20, \quad (9)$$

if the C axis is parallel to the boundaries.

From equations (2)-(9) it follows that at  $T \simeq 0.5T_c$  and  $L \simeq \xi_N^*$  the simple estimations for the parameter  $V_c$  are valid for the sandwich-type junctions

$$V_c \simeq 80\gamma_B^{-1} \text{ mV}, V_{c\parallel} \simeq 4 \text{ mV}, V_{c\perp} \simeq 10^{-2} \text{ mV} \quad (10)$$

and for the variable thickness bridges

$$V_c \simeq 80\gamma_B^{-3/2} \text{ mV}, V_{c\parallel} \simeq 1 \text{ mV}, V_{c\perp} \simeq 5 * 10^{-3} \text{ mV}. \quad (11)$$

From Eqs. (10) and (11) it follows that the suppression of the parameter  $V_c$  in HTS weak links is the result of the finite transparency of HTS/N-metal boundaries. It is also interesting to note that equations (2), (4) and (5), (6) determine the scaling law

$$V_c \propto R_N^{-k}, \quad (12)$$

where  $k = 1$  or  $k = 3$  for the sandwich type junctions and the variable thickness bridges respectively.

The theoretical predictions (2)-(12) can be easily used for interpretation of recent experimental results.

## 2.1 HTS/N/LTS sandwiches

These structures are usually used to investigate the quality of the HTS/N interface ( $N = \text{Ag, Au}$ ). Unfortunately the useful information is seriously

masked by the suppression of the superconductivity in the vicinity of the N/LTS boundary (LTS = Nb, Pb, Sn) since the parameter  $\gamma$  is greater or nearly equals unity here. In this case the value of the anomalous Green's functions responsible for the critical current have to be proportional to  $(T_c^* - T)$  at the interface and at  $T \simeq T_c^*/2$  their absolute value is an order of magnitude less than the order parameter of the bulk LTS electrode. Hence in the vicinity of the critical temperature  $T_c^*$  of LTS material the  $V_c(T)$  dependencies have to be proportional to  $(T_c^* - T)$  and the absolute value of parameter  $V_c$  be strongly suppressed [16].

These predictions fit well the experimental  $V_c(T)$  dependencies [17, 18]. To obtain better agreement with absolute values  $V_c \simeq 50 - 500$  mV it is necessary to assume that the order parameter near HTS/N interface is also suppressed ( $\Delta \simeq 0.1 - 1$  mV). This fact can be due to the ion cleaning of the HTS surface before the N film deposition leading to the formation of the thin oxygen deficient nonsuperconducting layer on the top of the film [13].

However even in the absence of such a layer the properties of HTS/N/LTS sandwiches seem to be close to those of SINS junctions where the role of I layer is played by this boundary. This is due to high  $\gamma_B$  values intrinsic to HTS/N boundaries. Recently, the scaling law  $I_c \propto R_N^{-1}$ , which is typical for SINS structures has, been proven experimentally in sandwiches YBCO/Ag/Nb [19].

## 2.2 Variable thickness bridges

The technology of the variable thickness bridges fabrication [2,3] usually starts with *in-situ* making the HTS/Ag,Au bilayers. The SNS junction is formed using high resolution lithography or ion milling to make a gap and then bridging this gap by Ag or Au.

Since the HTS films in all experimental realizations of the structures were C-oriented, the *in-situ* fabricated HTS/N boundary have a small transparency and the properties of the junctions were determined by the quality of the interface between the bilayer edges and the bridging film resulting in SNS sandwich type junctions. The experimental data [2] are fitted well by the theoretical predictions for SNS sandwiches following from equation (2) with  $\gamma_B = 20$ .

Using the typical value of  $2 \cdot 10^{-11} \Omega\text{cm}^2$  for the  $\rho_N \xi_N^*$  product and experimentally defined  $R_N \simeq 4\Omega$  (for the junctions made by means of the electron beam lithography) from (4) one can obtain the area  $A \simeq 5 \cdot 10^{-12} \text{ cm}^2$  for the real cross-section of the junction. The latter differs from the geometrical assessment by nearly two orders of magnitude. This discrepancy may be due to the oxygen diffusion during the fabrication

processes which extends preferably into the ab-planes than along the C-axis.

Thermal treatment of the bridges made by the ion milling method [2] increases the critical current of the junctions and decreases their normal resistance due mainly to the growth of the area  $A$  because of the normal metal diffusion process. The comparison of the data with the  $V_c(T)$  dependence given by equation (2) shows that this method of fabrication results in worse SN-boundary transparency ( $\gamma_B \simeq 250$ ) and lower  $V_c$ .

So the properties of the boundaries play a decisive role in these structures. To make these boundaries more controllable it is necessary to begin the Josephson junction fabrication with the deposition of the SN bilayers based on a-oriented films.

### 2.3. Edge-type junctions.

The technology of the junction fabrication usually begins with the deposition of the HTS/dielectric bilayers. Then a part of the structure is removed by ion milling to obtain the edge. Before the top electrode deposition the edge is exposed to a plasma discharge process in  $\text{CF}_4$  gas [4,5] or a thin PrBaCuO layer is grown [6].

The investigation of the junctions [4] shows that they reveal the Josephson-like behavior for the temperature  $T > 0.5T_c$ . A decrease of the temperature leads to intensive growth of the parameter  $V_c$  and to the shrinking of the Shapiro steps in the  $iv$ -curve. This behavior is typical for SS'S structures where the transition between depairing and the Josephson effects takes place when  $T$  passes through the critical temperature of the weak link material.

The experimental data obtained for the junctions with the PrBaCuO interlayer with the thickness  $d \simeq 6 \text{ nm}$  [6] are fitted well by the theoretical predictions for SNS junctions with rigid boundary conditions at SN interfaces [20] with  $d \simeq 6\xi_N^*$ . So we can conclude that the coherence length of the Pr-based compound ( $\simeq 1 \text{ nm}$ ) is close to that of YBCO material and the suppression of the parameter  $V_c$  in these structures is mainly due to the large value of the N-layer thickness.

The surface of the film edge in the above mentioned technique can be tormented during the process of the edge fabrication leading to an irreproducibility of the junction parameters. To circumvent this difficulty a new technique has been proposed [7]. First a sharp step in a substrate is produced. Then the HTS film is deposited across the step. The obtained superconducting electrodes are *in-situ* linked via the deposition of the normal metal film. The process results in a fabrication of the SNS sandwiches with different transparencies of the SN boundaries which can be characterized by the parameters  $\gamma_{B1}$  and  $\gamma_{B2}$ .

The theoretical analysis of the structure in the practically interesting case of the small electrode spacing leads to equation (2) in which the product  $0.5\gamma_B$  must be replaced by  $\gamma_B^* = \gamma_{B1}\gamma_{B2}/(\gamma_{B1} + \gamma_{B2})$ . It is important to note that in the limit  $\gamma_{B1} \gg \gamma_{B2}$  the stationary properties of the structure happen to be close to that of the SINS junction where the role of I-layer is played by the boundary with larger  $\gamma_B$ . In this case the characteristic voltage  $V_c$  depends only on  $\gamma_{B2}$  as for the symmetric SNS sandwiches. Thus to achieve the estimated  $V_c$  values (10) it is sufficient to have only one perfect SN boundary.

## 2.4. Sandwich-type junctions

Despite of the failure with PrBaCuO interlayers the idea of employing epitaxial trilayer structures for the Josephson junction fabrication is still promising. This has been confirmed by recent experiments with Nb-doped SrTiO<sub>3</sub> as the new coupling material which at the doping level between  $10^{17}$  and  $10^{20}$  cm<sup>-3</sup> is a good normal metal [8]. The experimental data obtained in these junctions with the N-layer thickness  $d \simeq 25$  nm are in a reasonable agreement with the predictions of the SNS junction's theory [20] with  $d \simeq 6\xi_N^*$ . The estimated value of coherence length  $\xi_N^* \simeq 5$  nm coincides with the estimations obtained in [8] from  $I_c(d)$  dependence.

So to get higher  $V_c$  values it is necessary to reduce the interlayer thickness.

## 3. Single grain boundary junctions

This type of junctions can be fabricated either by patterning the randomly occurring grain boundaries in granular films [9] or by epitaxial growth of the HTS films on the complex substrates (bicrystal [10], step-edge [11], or obtained by "planarization" technology [12]).

The scope of experimental data [9-12] (excess current in iv-curve, temperature dependence of  $V_c(T) \propto (T_c - T)^2$  at  $T \simeq T_c$ , the scaling law (11) with  $k \simeq 1$ ) permit to conclude that the junctions are of the SNS type. The only contradiction comes from the values of the normal resistance ( $10^{-7} - 10^{-8}$   $\Omega\text{cm}^2$ ). For SNS junctions this values would imply that the resistivity of the N-metal is about 0.2 to 2  $\Omega\text{cm}$  assuming a thickness of some 0.5 nm for the N-layer. This value of the resistivity is several orders of magnitude larger than that of the grain material.

The key to the problem can be found if we take into account the wave nature of the charge carriers. The estimations show that their de-

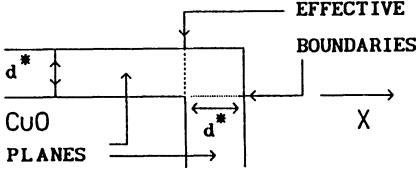


Fig.1. The scheme of the  $90^\circ$  grain boundary.

Brogile wavelength  $\lambda$  is comparable with the effective thickness  $d^*$  of their localization in the vicinity of CuO planes. So we have the effective waveguide for the carriers and any inhomogeneities of the scale  $d^*$  lead to diffraction and as a consequence to an additional resistance.

To calculate this resistance for the  $90^\circ$  grain boundary (see Fig.1) we suppose that the quasiparticles are localized within the conductive layer of thickness  $d^*$  and the probability of their tunneling to the neighboring layers is negligibly low. Assume also that the wave function equals to zero at the boundaries of the CuO planes and that the parameter  $\alpha = (2d^*/\lambda) \simeq 1$ .

Solving the Schrodinger equation we get the transparency coefficient

$$D(\theta) = 0, \quad \epsilon = \arccos(1/\alpha) > \theta > \pi/2, \quad (13a)$$

$$D(\theta) \simeq 7.5(\alpha^2 \cos^2(\theta) - 1), \quad 0 \leq \theta \leq \epsilon, \quad (13b)$$

where  $\theta$  is the angle between the Fermi-momentum of the quasiparticles and the X axis (see Fig.1).

To calculate the grain boundary resistance we solve master equations. Taking into account that  $D \ll 1$  and equation (13) for  $d^* \simeq 0.5$  nm one can obtain

$$R_N^{-1} = \frac{e^2 \alpha}{2\pi d^*} \int_0^{\pi/2} D(\theta) \cos(\theta) d\theta \simeq 5 * 10^3 (\alpha^2 - 1)^{3/2} \Omega^{-1} \text{cm}^{-1}. \quad (14)$$

Expression (14) fits the experimental data if

$$\alpha \simeq 1 + (1 - 5) * 10^{-3} \text{ or } \lambda \simeq 2d^* \simeq 1 \text{ nm}. \quad (15)$$

Thus the chosen value for  $\lambda$  is closed to that obtained by the other methods [15].

In the framework of the proposed waveguide model it is possible to explain the Josephson properties of the grain boundaries. They look like the SNS sandwich with two effective boundaries formed by the inhom-

geneities of the plane waveguide. The diffraction region between these boundaries serve as the weak link material. The calculation of the critical current in this model is in progress now.

#### 4. Conclusion

The analysis of the HTS Josephson junctions have shown that to understand their properties it is necessary to take into account the wave nature of the current carriers in the CuO planes. It is the diffraction of the quasiparticles that determines the specific resistance of the clean HTS/N-metal boundaries and hence the properties of the HTS weak links. The processes in single grain boundary junctions can also be understood in the framework of the waveguide model taking into account this effect.

#### 5. References

- [1] B.A. Aminov, A.I. Akimov, N.B. Brandt, Nguen Min Tchu, Ya.G. Ponamarev, M.V.Sudakova, J. Witting, L.M. Fisher, L. Rohta: *Physica C* **160**, 505 (1989)
- [2] M.G. Forrester, J. Talvacchio, J.R. Gavaler, J. Rooks, J. Lindquist: *IEEE Trans. Mag.* **27** 3098 (1991)
- [3] M.S. Wire, R.W. Simon, J.A. Luine, K.P. Daly, S.B. Coons, A.E. Lee, R. Hu, J.F.Burch, C.E.Platt: *IEEE Trans.Mag.* **27** 3106 (1991)
- [4] R.B. Laibowitz, R.H. Koch, A. Gupta, G. Koren, W.J. Gallager, V. Foglietti, B. Oh, J.M. Viggiano: *Appl.Phys.Lett.* **56** 686 (1990)
- [5] G. Koren, E. Aharony, E. Polturak, D. Cohen: *Appl.Phys.Lett.* **58** 634 (1991)
- [6] J. Gao, W.A.W. Aarnink, G.J. Gerritsma, H. Rogalla: *Physica C* **171** 126 (1990)
- [7] M.S. Dilorio, S. Yoshizumi, K-Y. Yang, J. Zhang, M. Maung: To appear in *Appl.Phys.Lett.* (1991)
- [8] D.K. Chin, T. van Duzer: *Appl.Phys.Lett.* **58** 753 (1991)
- [9] S.E. Russek, D.K. Lathrop, B.H. Moeckly, R.A. Buhrman, D.H. Shin, J. Silcox: *Appl.Phys.Lett.* **57** 1155 (1990)
- [10] R. Gross, P. Chaudhari, M. Kawasaki, M.B. Ketchen, A. Gupta: *IEEE Tran. Mag.* **27** 3227 (1991)
- [11] K.P. Daly, W.D. Dozier, J.F. Burch, S.B. Coons, R. Hu, C.E. Platt, R.W. Simon: *Appl.Phys.Lett.* **58** 543 (1991)
- [12] K. Char, M.S. Colclough, S.M. Garrison, N. Newman, G. Zaharchuk: To be published.



- [13] M.Yu. Kupriyanov, K.K. Likharev: Uspekhi Fiz. Nauk. [Sov. Phys. - Uspekhi] **160** 49 (1990)
- [14] M.Yu. Kupriyanov, K.K. Likharev: IEEE Trans. Magn. **27** 2460 (1991)
- [15] L.N. Bulaevskii, V.L. Ginzburg, A.A. Sobyenin: Zh.Eksp.Teor.Fiz. [Sov. Phys. - JETP] **94** 355 (1988)
- [16] M.Yu. Kupriyanov, V.F. Lukichev: Fiz.Nizk.Temp. (Sov. J. Low Temp. Phys.) **8** 1045 (1982)
- [17] H. Akoh, C. Camerlingo, S. Takada: Appl.Phys.Lett. **56** 1487 (1990)
- [18] M. Lee, D. Lew, C.B. Eom, T.H. Geballe, M.R. Beasley: Appl.Phys. Lett. **57** 1152 (1991)
- [19] A. Fujimaki, T. Tamaoki, T. Hidaka, M. Yanagase, T. Shiota, Y. Takai, H. Hayakawa: Japan.J.Appl.Phys. **29** L1659 (1990)
- [20] K.K. Likharev: Sov.Tech.Phys.Lett. **2** 12 (1976)